Imaging of the Cavernous Sinus

Nafi Aygun, MD, FACR[a,b,*], William K. Erly, MD, MBA[a,b], Joaquim M. Farinhas, MD, MBA[a,b]

KEYWORDS

• Cavernous sinus • High-resolution MR imaging • Pituitary adenoma • Tolosa-hunt syndrome

KEY POINTS

- Overlapping clinical and imaging manifestations of cavernous sinus (CS) pathologies require careful differential diagnosis.
- Identification of CS invasion by pituitary adenoma is critical to guiding treatment and heavily relies on high resolution MR imaging.
- Meningiomas and schwannomas of the CS can often be differentiated based on their high-resolution MR imaging features.
- Toloso-Hunt syndrome is a diagnosis of exclusion.
- Acute septic thrombosis of the CS is a rare life-threatening condition that radiologists should remember to include in their workup.

INTRODUCTION

The cavernous sinuses are complex anatomic crossroads where critical neurovascular structures traverse a confined dural space, making them uniquely vulnerable to a wide spectrum of pathologic processes. Lesions involving the cavernous sinuses often present significant diagnostic and therapeutic challenges because diverse etiologies, including neoplastic, inflammatory, infectious, and vascular disorders—can produce overlapping clinical manifestations and imaging appearances. A thorough understanding of cavernous sinus anatomy, patterns of cranial nerve involvement, venous drainage, and arterial relationships is therefore essential for accurate localization, differential diagnosis, and treatment planning. This article reviews the detailed anatomy of the cavernous sinus, correlates clinical presentations with underlying pathophysiology, and systematically discusses the imaging features of common and uncommon cavernous sinus pathologies, with an emphasis on practical distinctions that guide clinical management.

ANATOMY

The cavernous sinuses (CS) are paired venous spaces enclosed within dural layers on either side of the sella turcica. Bony borders of the CS include the tuberculum sella and the anterior clinoid process anteriorly, the posterior clinoid process posteromedially, the petroclival fissure posteroinferiorly.[1] The CS is laterally confined by the double layered dura of the middle cranial fossa. The superficial (meningeal, outer or lateral) layer covers the temporal lobe. The deep (inner or medial) layer envelops the oculomotor (CNIII), trochlear (CNIV), ophthalmic (CNVi), and maxillary (CNVii) nerves. The roof of the CS is made by a horizontal projection of the middle cranial fossa dura named as the transverse plate. The transverse plate attaches to the anterior and posterior clinoid processes and medially continues as the diaphragma sella. The medial wall of the cavernous sinus is made by a single layer of dura.[2] The floor of the CS is formed by the dura lining the greater wing of the sphenoid bone.

[a] Division of Neuroradiology, Department of Diagnostic Imaging, Moffitt Cancer Center, Tampa, FL, USA;
[b] Department of Oncological Sciences, University of South Florida, Tampa, FL, USA
* Corresponding author. Department of Oncological Sciences, University of South Florida, Tampa, FL.
E-mail address: Nafi.aygun@moffitt.org

Radiol Clin N Am 64 (2026) 707–718
https://doi.org/10.1016/j.rcl.2026.02.002

Abbreviations

AIFS	acute invasive fungal sinusitis
CCF	carotid-cavernous fistulas
CICA	cavernous internal carotid artery
CIFS	chronic invasive fungal sinusitis
CS	cavernous sinuses
FS	fungal sinusitis
ICA	internal carotid artery
IgG4-RD	immunoglobulin G4-related disease
ILT	inferolateral trunk
MHT	meningohypophyseal trunk
NHL	Non-Hodgkins lymphoma
PA	pituitary adenomas
THS	Tolosa-Hunt syndrome
VMs	venous malformations

The contents of the CS include endothelium lined fibrous septa that separate venous caverns, ligaments, the abducens (CNVI) nerve, the internal carotid artery (ICA), sympathetic ganglia and fat.[1] CNs III, IV, Vi and Vii are embedded withing the lateral wall of the CS (**Fig.1**). The intracavernous ligaments anchor the medial wall to the other walls and the ICA and are important structures in the context of transcavernous surgery but will not be further described here.

Along the posterior wall of the CS is a triangular area called the basin, which is bordered superiorly by the transverse plate, laterally by the petroclinoid folds (extensions of tentorium) and inferiorly by Meckel's cave. The CNIII and CNIV enter the CS through the basin.[1] The CNIII carries a 6 to 8 mm long pocket of arachnoid around it which is readily visible on MR imaging along the superior lateral margin of the CS. The CNVi and CNVii leave the Meckel's cave to enter the CS along its posterolateral margin. The CNVI exits the prepontine cistern by piercing the dural layers and travels through venous spaces (the basilar plexus and the

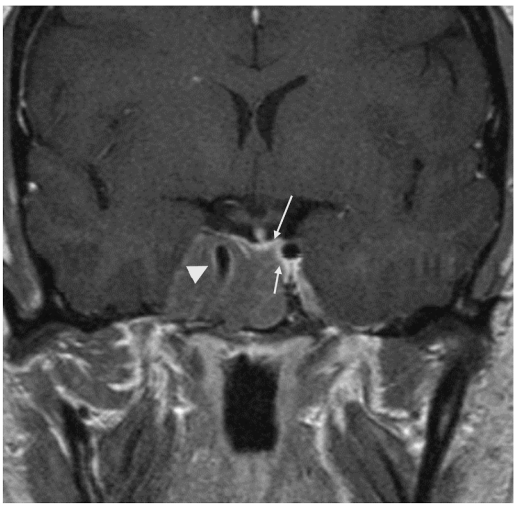

Fig. 2. Coronal contrast-enhanced T1W image through the sella shows a large PA infiltrating the right CS. The right cICA is completely encased but not narrowed (*arrowhead*). A small normal appearing pituitary gland is noted on the left (*long arrow*). The medial venous space in the left CS is maintained indicating no CS invasion (*short arrow*).

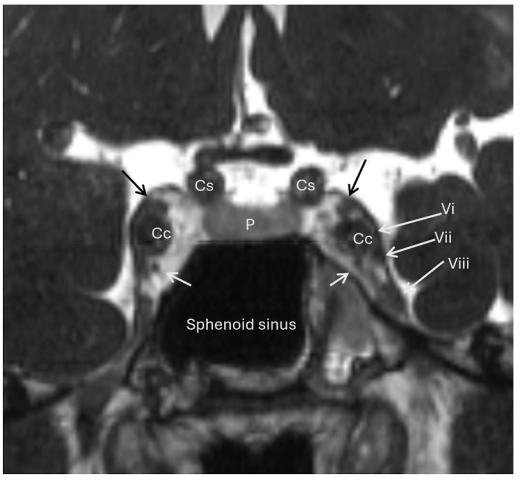

Fig. 1. Coronal contrast-enhanced CISS image through the CS. The CNVI (*short white arrow*) is surrounded by enhancing venous space. The CNIII (*black arrow*), ophthalmic (Vi) and maxillary (Vii) nerves are embedded within the lateral wall of the cavernous sinus. Cc, Cavernous ICA; Cs, Supraclinoid ICA; P, pituitary gland; Viii, Mandibular nerve.

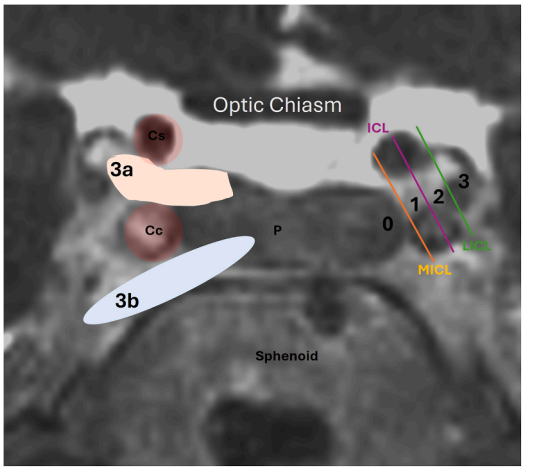

Fig. 3. Medial intercarotid (MICL), intercarotid (ICL) and lateral intercarotid (LICL) lines and Knosp's grades are superimposed on coronal CISS image. Grade 4 occurs when PA completely encircles the cICA as seen in **Fig. 2**.

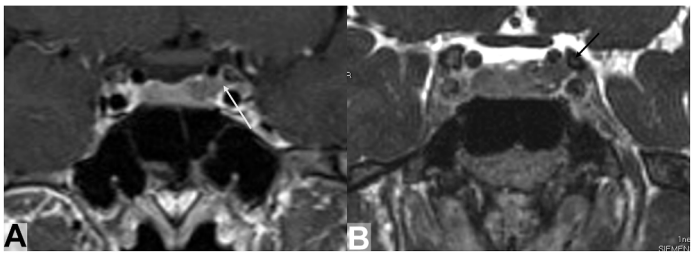

Fig. 4. Contrast-enhanced coronal T1W image (*A*) shows a small adenoma in the left lateral aspect of the pituitary with extension to the intercarotid line (*arrow*). Contrast-enhanced coronal CISS image (*B*) shows the lesion abutting the anterior clinoid process (*arrow*) implying grade 3a disease.

inferior petrosal sinus) before entering the cavernous sinus, usually below the ligament extending from the petrous apex to the dorsum sellae.[3] The CNVI carries dura, arachnoid and fibrous bands around it as it travels through the CS. All other cranial nerves travel anteriorly enclosed within the lateral wall of the CS and exit the CS through the superior orbital fissure.

The CS receives venous blood from the superior and inferior ophthalmic veins, sphenoparietal sinus, superficial middle cerebral vein and the pterygoid plexus of the masticator space and drains into the superior and inferior petrosal sinuses. The anterior and posterior intercavernous sinuses connect the right and left CS.

The branches of the cavernous ICA can be variable and most consistently include the meningohypophyseal trunk (MHT) and the inferolateral trunk (ILT). The MHT is located along the medial surface of the posterior genu and gives off branches to supply the posterior pituitary, clivus, cranial nerves, and the tentorium. The ILT arises as a single trunk or multiple vessels from the lateral surface of the cavernous ICA and supplies the adjacent dura and cranial nerves. Both ILT and MHT have extensive collaterals with each other and external carotid artery branches.

The persistent trigeminal artery, present in 0.2 %-0.4% of the population, serves as a conduit between the cavernous ICA (cICA) and the basilar artery. It travels in the CS within a course parallel to CN VI and leaves the CS through the dorsum sellae near Meckel's cave.

SYMPTOMS

Most patients with CS pathologies are symptomatic and most frequently present with progressive cranial neuropathy of the CNs II-IV. Visual impairment due to CNII compression and/or ischemia is common at presentation.[4] A thorough neuro-ophthalmologic assessment is essential and should include evaluation of the visual acuity, ocular mobility, facial and corneal sensation. Exophthalmos and chemosis may result from mass effect and compression of veins. While routine endocrinologic assessment is not indicated hormonal disturbance may be present in tumors of the CS and most frequently include hyperprolactinemia due to disturbance of the pituitary infundibulum.[5]

Cranial neuropathies can be isolated or multiple and include sympathetic and parasympathetic dysfunction. A specific combination of symptoms and examination findings may help pinpoint the exact anatomic location of the pathology as in orbital apex syndrome (ophthalmoplegia + vision loss + sensory loss in CNVi distribution), superior orbital fissure syndrome (ophthalmoplegia + sensory loss

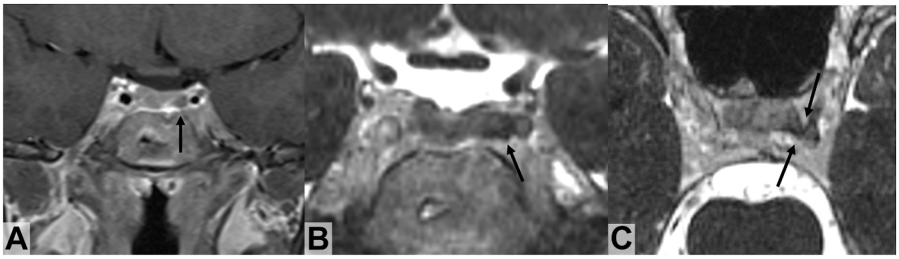

Fig. 5. Contrast-enhanced coronal T1W image (*A*) shows a small adenoma (*arrow*) in the left lateral aspect of the pituitary with the medial venous compartment of the CS being uneffaced, suggesting no CS invasion. Contrast enhanced coronal (*B*) and axial (*C*) CISS images reveal a tiny nubbin of tissue (*arrow*) protruding into the cavernous sinus. A small dural defect and CS invasion was found in surgery.

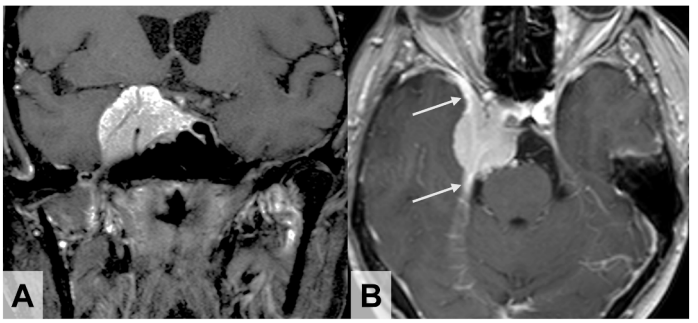

Fig. 6. Coronal (*A*) and axial (*B*) contrast-enhanced T1W images show a typical CS meningioma completely filling the CS and extending to the middle and posterior cranial fossa along dural reflections. Notice dural tails (*arrows*) and narrowing of the cICA.

in CNVi distribution) and cavernous sinus syndrome (ophthalmoplegia + sensory loss in CNVi and CNVii distributions + Horner's syndrome). However, it's difficult to ascertain etiology as many different pathologies give rise to similar symptoms and findings.

CAVERNOUS SINUS PATHOLOGIES

Neoplasms

Pituitary adenoma

In surgical series, up to 10% of pituitary adenomas (PA) are found to be invading the CS typically by violating the medial wall of the CS which is made of only a single layer of dura (**Fig.2**).[6] PAs invading the CS are the most common tumors of the CS. CS invasion by PA is a major predictor of incomplete surgical resection, failure to achieve remission in endocrinologically active PAs and recurrence thus presurgical recognition of CS invasion is important. Cottier and colleagues tested the hypothesis proposed by Knosp and colleagues by assessing PA relationship with the cICA on the coronal MR images as a predictor of CS invasion.[7,8] In their series CS invasion was found to be highly probable if (1) PA extended lateral to the lateral intercarotid line (tangent connecting the lateral edges of the cICA and supraclinoid ICA), or (2) PA encased greater than 67% of the cICA circumference or (3) PA effaced the carotid sulcus venous compartment (the venous space inferior to the cavernous cICA). There was no CS invasion if (1) PA did not extend lateral to the medial intercarotid line (tangent connecting the medial edges of the cICA and supraclinoid ICA) or (2) PA encased less than 25% of the cICA circumference.

Micko and colleagues further refined the Knosp classification and established a 6-tier probabilistic scheme for PA invasion of CS.[9] In this work, the medial, middle and lateral intercarotid lines differentiated 4 tiers with 2 additional tiers identified based on PA invasion inferior to the cICA and complete circumferential encasement of cICA (**Fig. 3**). Only 25% of the patients were assigned either the lowest (0) or the highest grade (4) which predicted 0% and 100% probability of CS invasion, respectively. The intermediate grades predicted an increasing likelihood of PA invasion with increasing grade, underscoring the difficulty of providing a definitive evaluation on preoperative MR imaging. One of the observations common in multiple surgical series is that even small microadenomas may invade the CS while the likelihood of CS invasion increases with increasing tumor size.

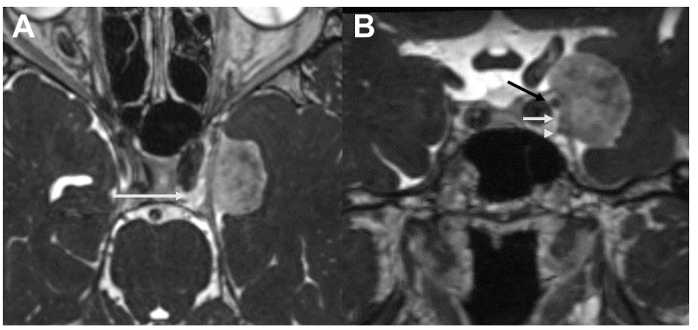

Fig. 7. Axial (*A*) and coronal (*B*) contrast-enhanced CISS images show a meningioma arising from the lateral wall of the left cavernous sinus which doesn't involve the CS proper (*arrow* in a). The CNIII (*black arrow*), CNVi (*white arrow*) and CNVii (*arrowhead*) are visible separate from the mass on image b. Surgical resection is feasible.

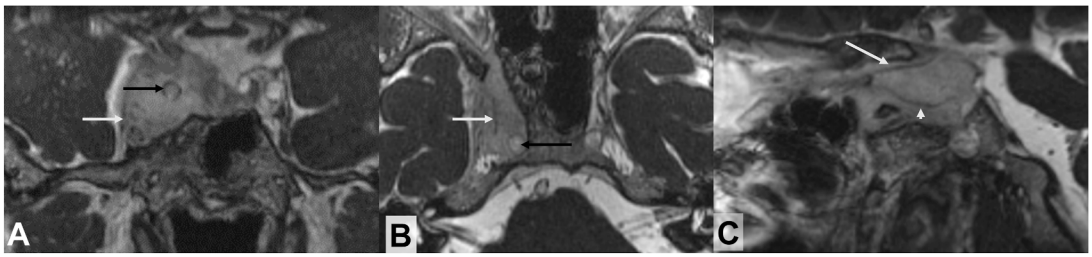

Fig. 8. Coronal (*A*) and axial (*B*) contrast enhanced CISS images show a meningioma completely filling the right CS and encasing the cICA (*black arrows*). Multiple nerve strands are visible within the mass (*white arrows*). Sagittal oblique reconstruction image (*C*) better depicts the CNIII (long *arrow*) and CNVii (*short arrow*) coursing through the mass. Surgical resection is not feasible.

To improve surgical outcomes new techniques such as endoscopic transcavernous approach and medial wall resection have been developed.[10] Intraoperative and histologic examination of the medial wall allowed identification of 3 distinct patterns of CS involvement: (1) Focal invasion, (2) Wall thickening, and (3) Wall destruction.[11] High resolution MR imaging of the pituitary has shown some success in identifying subtle forms of CS invasion preoperatively (**Figs. 4** and **5**).

Meningioma

Meningiomas are the most common primary tumors of the CS and make up to 40% of all CS tumors. They can arise from within the CS proper, CS walls or adjacent dura. When the CS proper is involved by meningioma, either primarily or by secondary invasion, curative surgery becomes unfeasible due to high rate of neurovascular complications (**Fig.6**).[12,13] Surgical resection of the extracavernous portion of meningioma followed by stereotactic radiotherapy targeting the residual CS component is a common treatment strategy in today's practice.[13,14] Imaging plays a critical role in surgical planning and differential diagnosis.[5] Encasement of the ICA and CNs is readily visualized on high resolution images. Meningiomas arising from the lateral wall and growing toward the middle cranial fossa are good surgical candidates (**Fig. 7**). A homogenously enhancing tumor infiltrating the CS and encasing the CNs is almost invariably a meningioma as other tumors tend to displace or replace the CNs (**Fig. 8**). Narrowing of the ICA by a CS tumor implies meningioma; although this finding is not always present in meningiomas it is rarely seen with other tumors. Hyperostosis in the adjacent bones and dural tail sign are other helpful imaging findings that point to meningioma although their absence would not necessarily exclude meningioma.

The posttreatment follow-up is straightforward in that any increase in size of the tumor implies treatment failure. A significant decrease in size of meningioma is not expected after radiotherapy. In fact, a significant decrease in size of tumor suggests nonmeningioma pathology. New CN deficit implies treatment failure as radiotherapy induced cranial neuropathy is rare in this setting. It is important to remember that clinical progression may precede imaging progression and that progression on imaging may be clinically silent.

The frequency of posttreatment imaging is dependent on factors such as symptoms, tumor grade, size etc. It is recommended to have more frequent imaging within the first 2 years of treatment.

Table 1
Differentiation of cavernous sinuses meningiomas from pituitary adenomas

Imaging Feature	Meningioma	Adenoma
Sellar enlargement	mild	marked
Pituitary gland visible	yes	no
Carotid narrowing	yes	no
Dural tail, hyperostosis	yes	no
Contrast enhancement	Avid, homogenous	Less, heterogenous
Tumor medial to precavernous ICA	no	yes

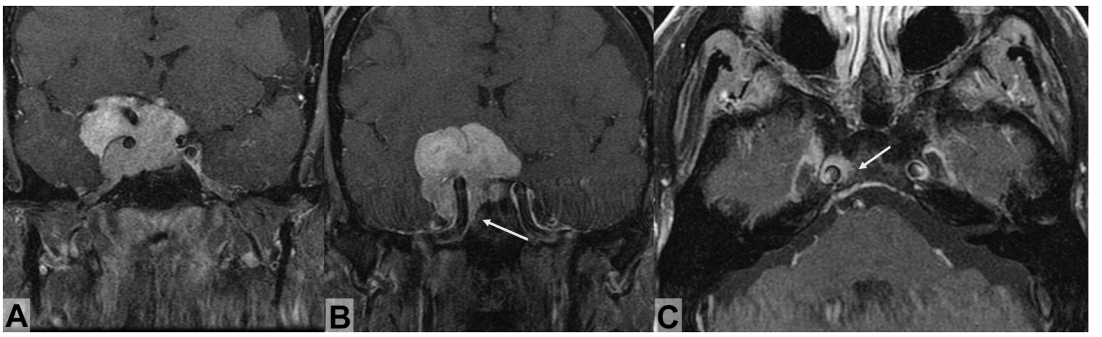

Fig. 9. Pituitary adenoma. Sella is markedly enlarged and the pituitary gland is completely replaced with tumor. The cICA is completely encased but not narrowed (*arrow* in b). Tumor extends medial to the ascending (precavernous or paraclival) segment of the ICA (*arrow* in c).

Differentiation of meningioma from macroadenoma Differentiating CS meningiomas invading the sella from large nonfunctioning macroadenomas invading the CS is a common challenge in radiologic practice, which has significant implications as the surgical approach may differ significantly.[5]

We found the imaging features listed in **Table 1** to be helpful in differentiating large sellar and parasellar meningiomas and PAs. Marked enlargement and remodeling of the sella is a reliable predictor of PAs as meningiomas usually cause less enlargement relative to tumor size. Most large adenomas obliterate the pituitary gland rendering it nonvisible on MR imaging. If even a small pituitary is identified a diagnosis of meningioma should be favored. Finding the infundibulum and following it to pituitary is a helpful method in this regard. Narrowing of a completely encased ICA is very suggestive of meningioma although this finding is only present in 1/3 of meningioma cases and may be present in some inflammatory conditions. Tumor extension medial to the precavernous (paraclival) ICA favors adenoma over meningioma (**Fig. 9**). It must be kept in mind that none of these findings have 100% predictive value. Statistically, a mass involving both the CS and sella is much more likely to be a PA than anything else. Thus, radiologists should have a high threshold for exclusion of PA.

Schwannoma

Schwannomas are the second most common primary tumors of the CS and most commonly arise from the CNV or CNIII. CNV schwannomas can have a dumbbell configuration with extension to the cisternal portion of the nerve whereas CNIII schwannomas can extend into the superior orbital fissure and orbit. They are usually well-circumscribed masses, which show prominent T2 hyperintensity and avid enhancement. Intratumoral cysts are frequently present. Schwannomas tend to replace the CN from which they arise on high resolution images in contrast to meningiomas, which encase the nerves (**Figs. 10** and **11**).

Surgical resection is the preferred treatment when feasible. Stereotactic radiotherapy is effective in stopping tumor growth.

Tumors secondarily involving the cavernous sinuses

Metastases Most commonly CS —metastasis occurs via perineural spread of head and neck cancers, which is discussed in *Cutaneous Lesions*

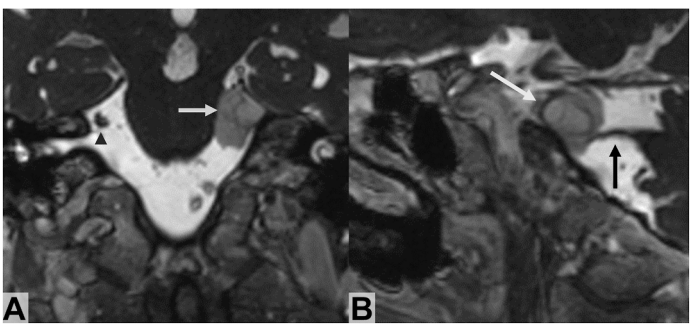

Fig. 10. Trigeminal schwannoma. Coronal (*A*) and oblique sagittal (*B*) contrast-enhanced CISS images show a mass in the left prepontine cistern extending to the CS (*white arrows*). The cisternal portion of the left CNV (*black arrow*) is not visible within the mass implying that the mass arises from the nerve and replaces it. Arrowhead points to the normal right CNV. Compare with **Fig. 11**.

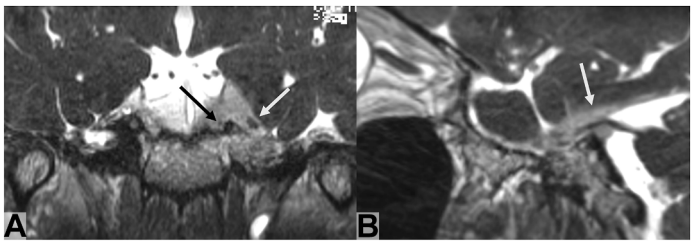

Fig. 11. Meckel's cave meningioma. Coronal (*A*) and sagittal oblique (*B*) contrast-enhanced CISS images show homogenously enhancing mass filling and expanding the left Meckel's cave. The CNV (*white arrows*) and CNVI (*black arrow*) are visible as they course through the mass. Compare with **Fig. 10**.

and Perineural Tumor Spread Involving the Orbit by Dr Kennemuth. Direct extension of skull base, orbit and paranasal sinus tumors to the cavernous sinuses is covered in *Skull base, bone, pituitary—regions around orbit that affect vision by Dr Houk*. Hematogenous metastasis to the CS is rare and usually seen in patients with metastatic disease elsewhere, posing no significant diagnostic challenge.

Lymphoma Non-Hodgkins lymphoma (NHL) may first present with cavernous sinus syndrome although isolated primary NHL of the CS is rare. Most cases of CS involvement by NHL represent direct extension from skull base and/or paranasal sinuses, which require differentiation from other infiltrative skull base tumors. An isolated CS lymphomatous mass usually shows homogenous enhancement, hypointense T2 signal compared with the cerebral cortex, decreased ADC values, and extension outside the CS along the cranial nerves (**Fig. 12**).[15] Inflammatory masses such as Tolosa-Hunt syndrome and IgG4-related disease may also have overlapping imaging and clinical features such as steroid responsiveness although the ADC values tend to be slightly higher.[15]

Cysts

Primary cystic masses in the CS are rare and include, arachnoid cysts, dermoid/epidermoid cysts, and neuroenteric cysts. These exhibit fluid signal on MR imaging and lack enhancing components. Dermoid cysts may contain mature fat tissue and epidermoids show increased diffusion

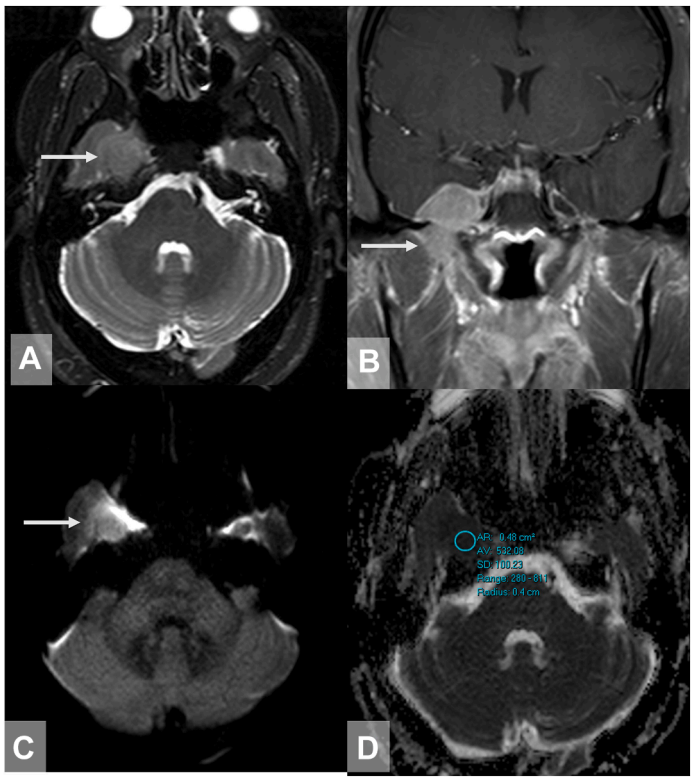

Fig. 12. Non-Hodgkin lymphoma in the right CS as the only site of disease. Well defined, T2 isointense to cerebral cortex mass filling and expanding the right CS and Meckel's cave (*A*) with homogenous contrast enhancement and extension through the foramen ovale to the masticator space (*B*). Increased DWI signal and low ADC values (~500) are noted (*C*, *D*).

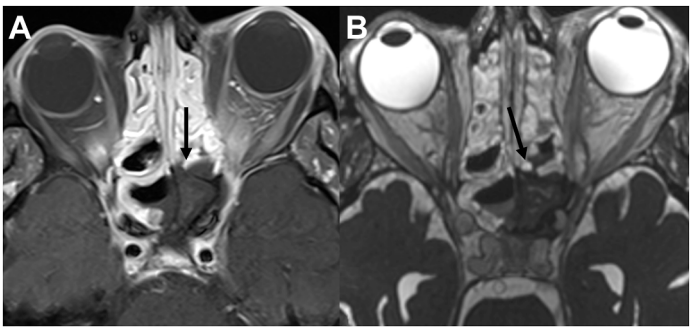

Fig. 13. (*A*, *B*) AIFS. Extensive mucosal inflammatory changes throughout the sinonasal cavity with lack of enhancement and T2 hyperintensity in the left posterior ethmoid and sphenoid sinuses indicate necrosis. Patient later developed CS thrombosis and intracranial complications.

weighted imaging (DWI) signal. Schwannomas in the CS are typically solid. While some schwannomas may contain cysts these are easily differentiated from primary cystic lesions by presence of an enhancing component.

Inflammatory Pathologies

Infections

Acute bacterial infections of the orbit, face and paranasal sinus can spread to the CS via venous flow and cause thrombophlebitis, which will be discussed in the next section. Common symptoms include headache and painful ophthalmoplegia. Acute thrombophlebitis of the CS must be differentiated from other inflammatory conditions.

Fungal sinusitis Among the various forms of fungal sinus infections, the acute invasive FS (AIFS), a disease of severely immunocompromised individuals, is notorious for its tendency to spread intracranially. CS involvement usually occurs via direct extension from the sphenoid or ethmoid sinuses and has a very high mortality rate. CS thrombosis, ICA thrombosis, ICA pseudoaneurysm formation, and rupture are among the most ominous imaging findings. Angioinvasion, the histopathological hallmark of AIFS, results in mucosal necrosis in the sinonasal fossa, which manifests as lack of enhancement on contrast-enhanced sequences (**Fig. 13**). This is known as the black turbinate sign when it involves the nasal turbinates. Erosion of the bony walls of the paranasal sinuses is characteristic of AIFS and helps differentiate other forms of sinusitis, although it is seen in the advanced stages of the disease.[16]

Chronic invasive FS (CIFS) is typically seen in moderately immunocompromised individuals and has a more protracted course than AIFS. CIFS usually presents with bone erosion and mass-like lesions inside and outside the sinonasal cavity and requires differentiation from malignant sinonasal tumors (**Fig. 14**). Vascular involvement may lead to catastrophic intracranial bleed or infarct.

Noninfectious inflammatory diseases

Tolosa-Hunt syndrome THS is a rare idiopathic inflammatory condition presenting with unilateral headache, ipsilateral painful ophthalmoplegia and -granulomatous- inflammation of the ipsilateral CS demonstrated by biopsy or MR imaging in the absence of other diseases that may account for the symptoms.[17] THS is a diagnosis of exclusion. There exists a broad overlap between clinical and radiologic features of THS and idiopathic orbital inflammation, idiopathic

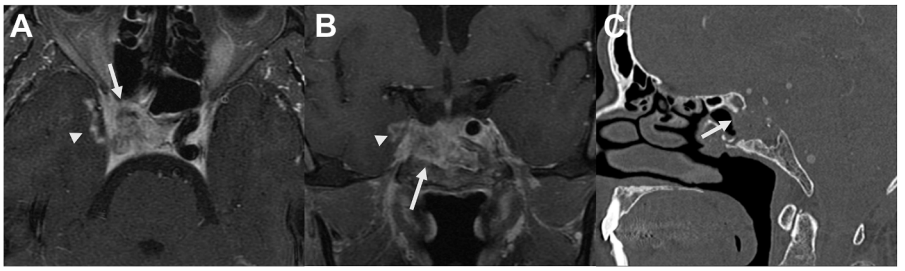

Fig. 14. CIFS. Heterogeneously enhancing tissue fills the right cavernous sinus (*arrows* in a and b). The right cICA is occluded. There is gyriform enhancement of the adjacent temporal lobe (*arrowheads* in a and b). Bone erosion (*arrow* in c) is frequently present in CIFS.

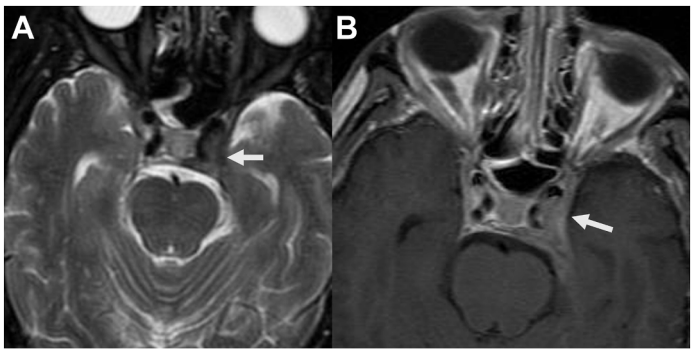

Fig. 15. THS. T2 hypointense (*A*) and enhancing (*B*) lesion in the left CS is demonstrated in a patient who presented with painful diplopia.

hypertrophic pachymeningitis, Immunoglobulin G4-related disease (IgG4-RD), cause specific CS inflammation such as sarcoidosis and infectious diseases such as tuberculosis and actinomycosis. MR imaging shows enhancing and T2 hypo-to-isointense tissue in the CS with possible extension to the orbit (Fig. 15). Narrowing of the cICA is present in about one-third of patients. Radiologic differential diagnosis of THS is broad and includes various tumors, infectious and inflammatory conditions of the CS.

THS responds to steroid treatment both clinically and radiologically although steroid responsiveness can also be present in some of its mimickers. Radiologic response may lag clinical response.

Immunoglobulin G4-related disease IgG4-RD is an immune triggered inflammatory process, which can affect multiple organs. Within the spectrum of entities, which can be seen in IgG4-RD, autoimmune pancreatitis, sclerosing cholangitis, lymphadenopathy, and salivary gland involvement are the most common. Orbital inflammatory conditions and retroperitoneal fibrosis are also relatively common. Vessel, thyroid gland, kidney, central nervous system, lung, and pleura involvement among others have been described. Establishing the diagnosis of IgG4-RD is difficult and requires convergence of clinical, radiologic and histopathological findings as well as exclusion of mimickers.[18] Serum IgG4 levels can be normal or elevated in IgG4-RD and in some of the clinical mimics. Likewise, IgG4 + plasmacytes in histopathologic specimens have limited utility. The most characteristic histopathologic features are storiform fibrosis, lymphoplasmacytic infiltrates, and obliterative phlebitis.

The most common CNS manifestation of IgG4-RD is hypophysitis followed by pachymeningitis. Dural based tumors may occur and the CS is a favored site for IgG4 related inflammatory pseudotumor (Fig. 16). They must be differentiated from other CS masses.

Neurosarcoidosis and *granulomatosis with polyangiitis* can involve the cavernous sinus either as a part of systemic disease or in rare cases in an isolated fashion. Diffuse thickening of the meninges and enhancement of the cranial nerves are common findings as in many other inflammatory conditions (Fig. 17). Nodular or mass-like appearance may also occur and require differentiation from tumors involving the CS.

Vascular Pathologies

Cavernous sinuses thrombosis

CS thrombosis is usually an acute and life-threatening condition that requires prompt

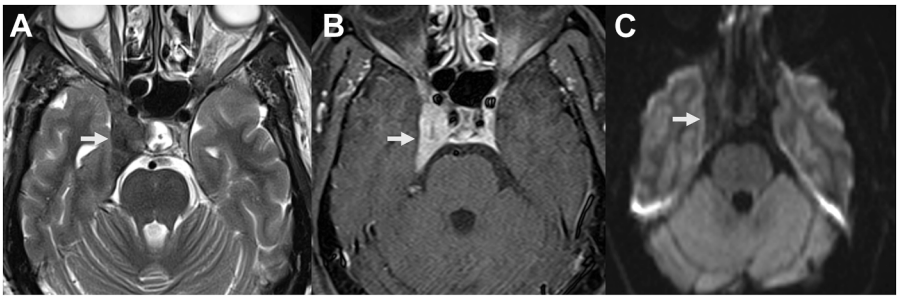

Fig. 16. IgG4-RD. T2 hypointense (*A*) and avidly enhancing (*B*) lesion in the right CS. Note the lack of increased DWI signal (*C*).

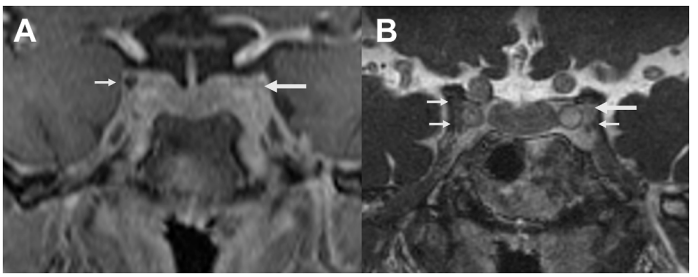

Fig. 17. Sarcoidosis of the left CNIII. Coronal contrast enhanced T1W image (*A*) shows non-visualization of the left CNIII (*long arrow*) with the normal right CNIII (*short arrow*) visualized as expected. Enhancement of the left CNIII renders it non-visible on the background of normal CS enhancement. Coronal contrast enhanced CISS image (*B*) shows a barely discernible swollen left CNIII (*long arrow*) and other normal cranial nerves (*short arrows*).

diagnosis and treatment. Most CS thromboses are septic and related to infections of the paranasal sinuses, orbit, face and temporal bone. Nonseptic thrombosis of the CS may be seen in the setting of dural venous thrombosis, but isolated nonseptic CS thrombosis is extremely rare. Headache is universally present and constant without response to symptomatic treatment. Fever is frequently present along with periorbital swelling and ophthalmoplegia.

Contrast-enhanced MR imaging and computerized tomography (CT) show bulging lateral contour of the cavernous sinus, intrasinus filling defects (thrombus) and enlarged superior ophthalmic veins (Fig. 18).[19] Indirect signs include findings of sinusitis, exophthalmos and stranding of the orbital fat. Thrombus may extend to the superior ophthalmic vein. Findings are frequently bilateral due to intracavernous venous communication although they can be unilateral early on. Infection may spread to the meninges and brain resulting in infarcts, meningitis, and abscesses.

Carotid-cavernous fistulas

Dural fistulas are acquired abnormal communications between the dural arteries and/or ICA and dural sinuses, meningeal or cortical veins. Carotid-cavernous fistulas (CCF) are traditionally divided to direct and indirect fistulas based on their arterial supply being from the ICA or meningeal vessels, respectively, although direct and indirect fistulas are etiologically and clinically distinct. Direct CCF usually occurs after trauma in young males and present with acute and severe symptoms whereas indirect CCF typically occur in postmenopausal women and present with insidious symptoms. Indirect CCF is thought to develop after CS thrombosis. The diagnosis of CCF is established with catheter angiography. MR imaging and CT show enlargement and abnormal contour of the CS, flow voids in the CS, enlarged intraorbital and cortical veins, orbital edema and extraocular muscle swelling.[20] Apparent enlargement of the CS may be seen in the setting of carotid tortuosity, atherosclerosis and suboptimal patient positioning and should be considered in the differential diagnosis of CCF.

Venous malformations

Venous malformations (VMs) (a.k.a. hemangioma) are rare CS tumors, which are histologically identical to common venous malformations that occur in other parts of the body. Like VMs elsewhere they exhibit marked T2 hyperintensity, gradual contrast enhancement extending from periphery to the center on dynamic contrast enhanced MR imaging and accumulation of ^{99m}Tc pertechnetate–labeled red blood cells on nuclear medicine examinations.[21] CS VMs are usually large at the time of diagnosis

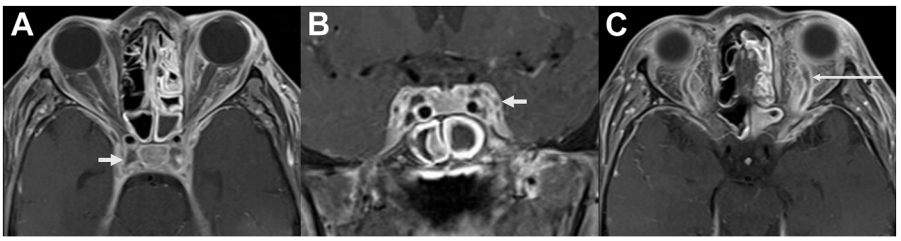

Fig. 18. CS thrombosis. Axial (*A*) and coronal (*B*) contrast-enhanced T1W images show slight expansion of the cavernous sinuses with multiple bilateral filling defects (*short arrows*). Note marked stranding of the orbital fat and paranasal sinus inflammatory change. Axial contrast-enhanced T1W image (*C*) shows thrombosis of the bilateral superior ophthalmic veins (*long arrow*).

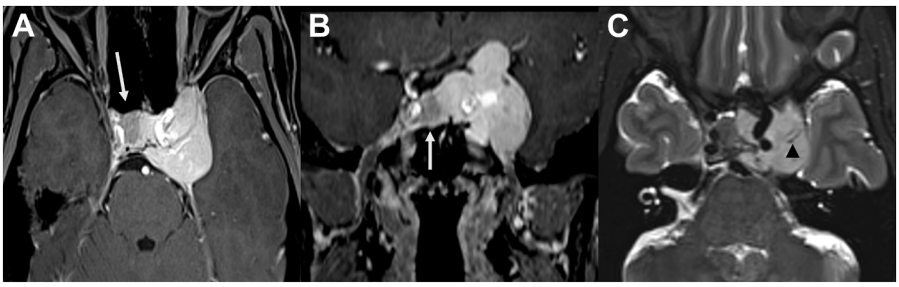

Fig. 19. VM (a.k.a hemangioma). A large, lobulated mass in the left CS and sella turcica with avid enhancement (*A*, *B*) and T2 hyperintensity (*C*) suggests PA although preservation of the pituitary gland (*arrows*) argues strongly against PA. Flow voids (*arrowhead* in c) indicate a hypervascular mass.

and present with symptoms related to mass effect (**Fig. 19**). Stereotactic radiotherapy is effective and preferred over surgery due to risk of excessive hemorrhage.[22]

Aneurysms

A through discussion of CS aneurysms is beyond the scope of this text. Most CS aneurysms are incidentally found and asymptomatic. Great majority of CS aneurysms do not require treatment. Most common symptom is CN palsy related to mass effect. CS aneurysms rarely rupture and may result in nonlife threatening CCF or epistaxis. Subarachnoid hemorrhage from spontaneous rupture of CS aneurysms is extremely rare.

SUMMARY

Pathology of the cavernous sinus encompasses a broad and heterogeneous group of conditions that reflect the complex anatomy and critical neurovascular contents of this region. Accurate diagnosis relies on careful integration of clinical presentation—particularly patterns of cranial neuropathy—with high-resolution imaging that delineates lesion location, extent, and behavior relative to the cavernous sinus walls, cranial nerves, and internal carotid artery. While many disease entities share overlapping imaging and clinical features, recognition of key distinguishing characteristics allows meaningful narrowing of the differential diagnosis and guides appropriate management strategies.

CLINICS CARE POINTS

- Extension of pituitary adenoma to cavernous sinus significantly diminishes prognosis.
- High resolution MRI helps guide surgical and non-surgical approcaches to CS meningiomas.
- A CS mass in a patient with history of head and neck cancer should be regarded as perineural spread of tumor.

DISCLOSURE

The authors have nothing to disclose.

REFERENCES

1. Lang J. Skull base and related structures : atlas of clinical anatomy. 2nd edition. New York: Schattauer; 2001. p. 338, xiii.
2. Lefevre E, Dupont S, Liguoro D, et al. Anatomy of the medial wall of the cavernous sinus: a systematic review of the literature. Clin Anat 2024;37(8):910–24.
3. Kshettry VR, Lee JH, Ammirati M. The Dorello canal: historical development, controversies in microsurgical anatomy, and clinical implications. Neurosurg Focus 2013;34(3):E4.
4. Hall WA, Gurnani B. Compressive optic neuropathy. In: StatPearls [Internet]. Treasure Island (FL): StatPearls Publishing; 2026.
5. Kwancharoen R, Blitz AM, Tavares F, et al. Clinical features of sellar and suprasellar meningiomas. Pituitary 2014;17(4):342–8.
6. Truong HQ, Lieber S, Najera E, et al. The medial wall of the cavernous sinus. Part 1: surgical anatomy, ligaments, and surgical technique for its mobilization and/or resection. J Neurosurg 2019;131(1):122–30.
7. Knosp E, Steiner E, Kitz K, et al. Pituitary adenomas with invasion of the cavernous sinus space: a magnetic resonance imaging classification compared with surgical findings. Neurosurgery 1993;33(4):610–7 [discussion: 617–8].
8. Cottier JP, Destrieux C, Brunereau L, et al. Cavernous sinus invasion by pituitary adenoma: MR imaging. Radiology 2000;215(2):463–9.
9. Micko AS, Wohrer A, Wolfsberger S, et al. Invasion of the cavernous sinus space in pituitary adenomas: endoscopic verification and its correlation with an MRI-based classification. J Neurosurg 2015;122(4):803–11.
10. Cohen-Cohen S, Gardner PA, Alves-Belo JT, et al. The medial wall of the cavernous sinus. Part 2: selective medial wall resection in 50 pituitary adenoma patients. J Neurosurg 2019;131(1):131–40.

11. Constanzo F, Rychen J, Lee CK, et al. Patterns of invasion of the medial wall of the cavernous sinus by pituitary adenomas. J Neurosurg 2025;143(4):895–906.
12. Pamir MN, Kilic T, Bayrakli F, et al. Changing treatment strategy of cavernous sinus meningiomas: experience of a single institution. Surg Neurol 2005;64(Suppl 2):S58–66.
13. Corniola MV, Roche PH, Bruneau M, et al. Management of cavernous sinus meningiomas: consensus statement on behalf of the EANS skull base section. Brain Spine 2022;2:100864.
14. Beer-Furlan A, Priddy BH, Jamshidi AO, et al. Improving function in cavernous sinus meningiomas: a modern treatment algorithm. Front Neurol 2020;11:652.
15. Ren J, Yuan Y, Wu Y, et al. Differentiation of orbital lymphoma and idiopathic orbital inflammatory pseudotumor: combined diagnostic value of conventional MRI and histogram analysis of ADC maps. BMC Med Imaging 2018;18(1):6.
16. Ilica AT, Mossa-Basha M, Maluf F, et al. Clinical and radiologic features of fungal diseases of the paranasal sinuses. J Comput Assist Tomogr 2012;36(5):570–6.
17. IHS classification ICHD-3 Tolosa-Hunt Syndrome. International Headache Society 2021.
18. Wallace ZS, Naden RP, Chari S, et al. The 2019 American College of Rheumatology/European League against Rheumatism classification criteria for IgG4-related disease. Ann Rheum Dis 2020;79(1):77–87.
19. Bhatia H, Kaur R, Bedi R. MR imaging of cavernous sinus thrombosis. Eur J Radiol Open 2020;7:100226.
20. Kim D, Choi YJ, Song Y, et al. Thin-Section MR imaging for carotid cavernous fistula. AJNR Am J Neuroradiol 2020;41(9):1599–605.
21. Benson JC, Eschbacher KL, Raghunathan A, et al. Cavernous Sinus vascular venous malformation. AJNR Am J Neuroradiol 2022;43(1):19–23.
22. Wang X, Mei G, Liu X, et al. The role of stereotactic radiosurgery in cavernous sinus hemangiomas: a systematic review and meta-analysis. J Neuro Oncol 2012;107(2):239–45.